

## Adsorption Behaviour of Reactive Black Dye 5 by Magnetically Separable Nano-adsorbent

M. Hamzehloo\*, B.K.A. Farahani and R. Rostamian

*Department of Physical Chemistry, School of Chemistry, University College of Science, University of Tehran, Tehran 14155, Iran*

*(Received 17 May 2019, Accepted 17 June 2019)*

Dyes in the textile industry are the most significant source of pollutants, which cause damaging effects to people's health. Reactive black 5 (RD5) is an anionic color that is currently used in the textile industry. This study is designed to provide the strategies to synthesize and characterize the new family of functionalized magnetite nanoparticles *via* a chemical co-precipitation method with polyaniline modification groups on the surface. The effect of various parameters including pH, the initial concentration of RD5, the mass of adsorbent, contact time, temperature and ionic strength has been studied. Under optimal conditions, 10 ml of RD5 solution with a concentration of 30 mg l<sup>-1</sup>, 20 mg of adsorbent, pH of 7 and contact time of 10 min, the color was completely removed. The results also showed that adsorption of RD5 followed Langmuir isotherm ( $R^2 = 0.998$ ) and the maximum RD5 adsorption capacity was 63.69 mg g<sup>-1</sup>. The results of kinetic studies also showed that the RD5 removal followed the pseudo-second-order equation with the correlation coefficient of  $R^2 = 0.9984$ . The  $\Delta G^\circ$  was negative at all temperatures which shows that the adsorption process was spontaneous. Conforming to our results, adsorption process by designed magnetic nano-adsorbent is an efficient and affordable method for eliminating RD5 from the textile industry.

**Keywords:** Reactive Black 5, Isotherm models, Kinetics, Magnetic adsorbent, Diffusion

### INTRODUCTION

Water is one of the most abundant compounds on the earth and the primary source of life, as we know today. Unfortunately, due to the current ignorance, changes in the quality of water have increased [1-4]. Dye is one of the main characteristics of surface water, which is essential due to the increase of the chlorine intake [5]. The presence of dye in water increases the potential for the formation of Trihalomethanes, the productive compounds of which can be deposited again in the environment. Industrial effluent from the textile industry and dye factories, paper production, food industry, chemical production, and ore extraction may release dyes in rivers and natural streams [6]. Thus, it is an important issue to treat surface water. Considering the capabilities of nanotechnology in comparison with the traditional methods, the removal of

environmental pollution can be regarded as green technology and a useful tool for achieving sustainable development, both economically and concerning productivity [7]. The presence of this technology in the field of environmental engineering and its practical application, especially in the area of wastewater treatment and creating the necessary conditions for the reuse of treated wastewater, is essential for the context of the water crisis. Among the various contaminations of our ecosystem, dyes are the largest and most important group of pollutant chemical series [8]. They are widely used in the textile, paper, plastics, and cosmetics industry. It should also be emphasized that several dyes are used in dyeing processes. Therefore, the dye in industrial effluent and surface water sources causes contamination. Even at low concentrations, dyes can be detected, while affecting the life and food of animals. The effect of removing dye from contaminated water is of great importance and has also received considerable attention in research and technology in recent

\*Corresponding author. E-mail: majhamzehloo@ut.ac.ir

years. Among the dyes, dyes have an “azo” functionalization categories, as water-soluble dyes are the most problematic dyes. Usually, a combination of different methods is needed to remove them. Adsorption is one of the essential techniques in removing dyes from contaminated water which is generally preferred to other ways, due to additional features such as fastness, simplicity, low cost, non-toxic, simple design, and high-efficiency performance [9]. The key factor in adsorption phenomena is to select an optimum adsorbent with the highest capacity as well as the fastest kinetics for pollution removal [2].

Different adsorbents are used to remove dyes, some of which include magnetic nanoparticles, natural adsorbents, activated carbon [10], silica gel, sawdust, peat, ash, bentonite, cellulose phosphate, and chitosan [11]. Magnetic nanoparticles have a couple of specific properties, such as the ease of synthesis of nanoparticles, large surface area, with a superparamagnetic property that makes these particles respond to external magnetic field and, in the absence of external field, lose their magnetic properties; they don't need the filtration process and centrifuge steps during the extraction process and the ability to extract large volumes of samples and removal of various organic and inorganic environmental pollutants [12]. Magnetite ( $\text{Fe}_3\text{O}_4$ ) has the highest magnetic properties in the iron oxides family, and that is why many studies have been implemented on the synthesis and application of these nanoparticles. In the absence of any surface coating, magnetic nanoparticles have a large surface-to-volume ratio and thus accumulation will be done to reduce their superficial energy and form large clusters that increase their size. Due to the interaction between the magnetic nanoparticles, the magnetic properties of each particle are enhanced by the magnetic field of the adjacent particle as a result of which their aggregate properties increase.

One of the protective methods of magnetic nanoparticles is creating a core-shell structure, in which the uncoated nanoparticles are a nucleus that is separated by a shell from the environment. The coatings shell can include coating with organic compounds including surfactants and polymers, coating with inorganic compounds including silica, carbon and precious metals (such as silver and gold). To stabilize magnetic nanoparticles, strong repulsive forces must overcome the magnetic interaction of particles

between particles as well high energy of surfaces [13]. This stabilization can be achieved through spatial repulsion or electrostatic repulsion. Thus, magnetic nano-adsorbents properties can be entirely designed by using functionalized polymers to enhance surface properties. One of the conducting polymers that have been researched in this field is polyaniline that presents an excellent efficiency in the removal of pollution [14]. According to the mentioned issue in this work, functionalized polyaniline on  $\text{Fe}_3\text{O}_4$  nanoparticles was synthesized, then implemented as an adsorbent for removal of RD5. The factors that influenced adsorption yield including pH of the solution, contact time of interaction and initial RD5 concentration, have been investigated. Adsorption isotherm, kinetic and thermodynamic parameters have been calculated from experimental data. These results could improve our knowledge about RD5 adsorption mechanisms to the high-efficiency design of the water treatment process.

## MATERIALS AND METHODS

### Preparation and Characterization of Core-shell Magnetic Adsorbent ( $\text{Fe}_3\text{O}_4@\text{PANI}$ )

All chemicals were purchased from Merck Company and used in analytical grade without any further purification. All aqueous solutions were made with double distilled water. Stock solutions of RD5, ( $\text{C}_{26}\text{H}_{21}\text{N}_5\text{Na}_4\text{O}_{19}\text{S}_6$ , see Figs. 1a and 1b) were prepared by dissolving it in deionized water. The pH of the solution was adjusted to the desired value using appropriate concentrations of HCl or NaOH solutions.

$\text{Fe}_3\text{O}_4$  nanoparticles were prepared by a chemical co-precipitation method [15]. Then, one gram of dried  $\text{Fe}_3\text{O}_4$  was mixed with 0.5 ml aniline monomer and mechanically blended for 5 min. Then, 20 ml of 0.2 molar sulfuric acid solution was added to this mixture. In the next step, 20 ml of ammonium peroxide solution (5 mM) was added dropwise to the mixture under stirring. After that, the mixture was stirred continuously for 2 hours and allowed to stand for one day at the same conditions. Finally, after 24 h, the product (abbreviated here as  $\text{Fe}_3\text{O}_4@\text{PANI}$ ) nanoparticles were washed several times with deionized water and ethanol and separated by an external magnet and dried in an oven at 70 °C for 5 h. Scanning electron

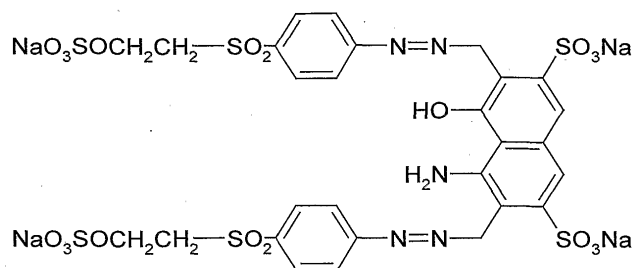


Fig. 1. The molecular structure of RD5.

microscopy (SEM) images were recorded by a TeScan-Mira III microscope. Fourier transforms infrared (FTIR) spectra were recorded by a Nicolet Magna 550 spectrometer using KBr pellet.

### Batch Adsorption Experiments

First, 30 ppm RD5 concentration was prepared and the pH of the solution was adjusted to 3, 5, 7, 9 and 11 using HCl and NaOH 10% (Vol) solution. After that, 10 mg of  $\text{Fe}_3\text{O}_4@\text{PANI}$  was added separately to each solution and shaken mechanically. Then, the samples were magnetically separated from the solution using a permanent magnet [3]. The residual RD5 concentrations in the solutions were measured using UV-Vis spectrophotometer (UV-Vis spectrophotometer Specord 250, Analytik Jena AG).

30 ppm RD5, 10 ml of RD5 and different masses of  $\text{Fe}_3\text{O}_4@\text{PANI}$  were used in every batch experiment and optimum pH value. Shaker was used to blend the mixture of adsorbent-adsorbate which were used for all the tested conditions. Then, the samples were magnetically separated and measured using UV-Vis spectrophotometer.

The experiment was implemented using 30 ppm RD5, 10 ml of RD5 and 2 mg of  $\text{Fe}_3\text{O}_4@\text{PANI}$  in every batch experiment and optimum pH value.

The thermodynamic parameters that must be considered to determine the process are changes in standard enthalpy ( $\Delta H^\circ$ ), standard entropy ( $\Delta S^\circ$ ), and standard free energy ( $\Delta G^\circ$ ) due to transfer of the unit mole of the solute from the solution onto the solid-liquid interface. The value of  $\Delta H^\circ$  and  $\Delta S^\circ$  were computed using the following equation:

$$\Delta G^\circ = \Delta H^\circ - T\Delta S^\circ \quad (1)$$

$$\Delta G^\circ = -RT\ln(K) \quad (2)$$

Rearranging Eqs. (1) and (2) gives Eq. (3) as follow. The value of  $\Delta H^\circ$  and  $\Delta S^\circ$  were computed using the following equation:

$$\ln(K) = \frac{\Delta S^\circ}{R} - \frac{\Delta H^\circ}{R} \frac{1}{T} \quad (3)$$

$K$  is the distribution coefficient which can be calculated as  $K = K_d = q_e/C_e$  [4].

The effect of ionic strength on adsorption capacity was investigated by increasing sodium chloride in the range of 0-5% percent (mass NaCl/mass solution) to each solution with 30 ppm RD5 concentration. 20 mg of  $\text{Fe}_3\text{O}_4@\text{PANI}$  was added separately to each solution and shaken thoroughly. Then, the samples were separated and measured.

The kinetic experiments were implemented in a batch mode with RD5 solutions of  $\text{Fe}_3\text{O}_4@\text{PANI}$  with 30 ppm of RD5 at optimized pH mixed and allowed to interact at various contact times [16]. Then, the samples were magnetically separated and the residual RD5 in the solutions was measured using UV-Vis spectrophotometer. The quantity of adsorption capacity  $q_t$  ( $\text{mg g}^{-1}$ ) was calculated using this equation:

$$q_t = \frac{(C_0 - C_t)}{W} \times V \quad (4)$$

where  $C_0$  is the initial RD5 concentration ( $\text{mg l}^{-1}$ ) and  $C_t$  is the remaining RD5 ( $\text{mg l}^{-1}$ ) at time  $t$ ,  $V$  is the volume of RD5 solutions (l) and  $W$  is the adsorbent amount (g).

Mathematical models such as the pseudo-first-order and pseudo-second-order model were applied to simulate the kinetic sorption data of RD5 [3].

In adsorption systems, thermodynamic data can only provide information on the equilibrium state of the system, such as adsorption capacity, while kinetic data consider the change in the chemical properties of a material over time. Using kinetic measurements, we can determine the kinetic constants of the adsorption process. It seems that the prediction of the rate of adsorption process is the most essential factor in the design of these systems. Recently, some efforts have been made to justify the kinetic adsorption mechanism by examining some adsorption processes in the removal of pollutants from the environment, and the results of these studies have been presented in several kinetic models in recent. The sorption dynamics were tested with the Lagergren (pseudo-first order) and pseudo-second order model. The linearized form of the pseudo-first order equation (Lagergren) is generally expressed as follows:

$$\ln(q_e - q_t) = \ln q_e - k_1 t \quad (5)$$

where  $q_e$  and  $q_t$  are the adsorption capacity at equilibrium and at time  $t$ , respectively ( $\text{mg g}^{-1}$ ) and  $k_1$  ( $\text{min}^{-1}$ ) is the rate constant of pseudo-first order adsorption.

The pseudo-second order kinetic model is represented by the following equation:

$$\frac{t}{q_t} = \frac{1}{k_2 q_e^2} + \frac{1}{q_e} t \quad (6)$$

where  $q_e$ ,  $q_t$  and  $t$  have the same meaning as explained above.  $k_2$  ( $\text{g mg}^{-1} \text{min}^{-1}$ ) is the overall rate constant of pseudo-second order sorption [17].

### Adsorption Isotherm Study (Effect of Concentration of RD5)

Dye's solution was prepared by diluting the stock solution in the range of 20-150  $\text{mg l}^{-1}$ . 10 ml of RD5 and 0.0020 g of  $\text{Fe}_3\text{O}_4@\text{PANI}$  was used in every batch experiment. Shaker was used to blend the mixture of adsorbent-adsorbate were used for all tested conditions. Then, the samples were separated like previous by UV-Vis

spectrophotometer. Adsorption isotherms present adsorption equilibrium state, by plotting equilibrium concentration versus the mass of the contaminant removed per mass  $\text{Fe}_3\text{O}_4@\text{PANI}$  ( $q_e$ ). The value of  $q_e$  can be calculated as presented in Eq. (7):

$$q_e = \frac{(C_0 - C_e)}{m} \times V \quad (7)$$

where  $q_e$  is the RD5 adsorption capacity ( $\text{mg/g}$  adsorbent),  $C_0$  is the initial concentration of RD5 ( $\text{mg l}^{-1}$ ),  $C_e$  is the RD5 concentration at the equilibrium found in the solution ( $\text{mg l}^{-1}$ ),  $m$  is the mass of  $\text{Fe}_3\text{O}_4@\text{PANI}$  (g) and  $V$  is total volume of solution (l) [3].

### Adsorption Isotherm Models

In general, adsorption isotherm models are applied to show the adsorption equilibrium results in different model conditions [2]. Adsorption models show the distribution of adsorption molecules in the liquid and solid phase when the equilibrium is reached. The experimental data obtained in the adsorption conditions will be determined from a specific isotherm model. The relationship between the amount of adsorbed material ( $q$ ) and its concentration in the fluid phase ( $C$ ) at temperature  $T$  is called adsorption isotherm at temperature  $T$ . In the current study, two isotherm models were implemented to investigate the adsorption phenomena.

Langmuir isotherm is applicable when the extent of adsorbate coverage is limited to one molecular layer [14]. This isotherm equation is expressed by Eq. (8):

$$\frac{C_e}{q_e} = \frac{1}{q_m} C_e + \frac{1}{K_L q_m} \quad (8)$$

In all isotherms and here,  $q_e$  ( $\text{mg g}^{-1}$ ) and  $C_e$  ( $\text{mg l}^{-1}$ ) are the amounts of adsorbed adsorbate per unit weight of adsorbent and equilibrium RD5 concentration in solution,  $q_m$  ( $\text{mg g}^{-1}$ ) is the maximum amount of adsorbed RD5 per unit weight of adsorbent and  $K_L$  ( $\text{l mg}^{-1}$ ) is the adsorption equilibrium constant. The empirical Freundlich model based on adsorption on a heterogeneous surface is given below by Eq. (9).

$$\log(q_e) = \log(K_F) + \frac{1}{n} \log(cc_e) \quad (9)$$

where  $K_F$  and  $n$  are the Freundlich constants.  $K_F$  and  $n$  are indicators of adsorption capacity and adsorption intensity, respectively [4].

## RESULTS AND DISCUSSION

### Characterization of the Adsorbent

In Fig. 2a, the synthesized  $\text{Fe}_3\text{O}_4$  has been depicted. This image shows that the magnetite nanoparticles have a spherical shape and the particle size of the product is in the range of 40-60 nanometers.

The crystalline structure of the magnetite  $\text{Fe}_3\text{O}_4$  nanoparticles were investigated by X-ray diffraction (Fig. 2b). The diffraction peaks are located at 30.300, 35.675, 37.160, 43.300, 57.175, 62.900, 71.290 related to the crystalline structure of 220, 311, 400, 422, 511, 440, 620 well recognized from XRD pattern.

The infrared spectrum of the magnetite  $\text{Fe}_3\text{O}_4$  nanoparticles is shown in Fig. 2c. FT-IR spectra were measured on a spectrophotometer under ambient conditions in a range of 400-4000  $\text{cm}^{-1}$  with a spectral resolution of 4  $\text{cm}^{-1}$ . To confirm the structure of the samples FT-IR spectrum was recorded at room temperature. The strong absorption band in low-wavelengths ( $<700 \text{ cm}^{-1}$ ) is assigned to vibration of the Fe-O functional groups. Two peaks at about 3420  $\text{cm}^{-1}$  and 2361  $\text{cm}^{-1}$  come from the hydroxyl group (OH) and  $\text{CO}_2$  present in the atmosphere. The presence of magnetite with three adsorption spectra is proved at 578, 690 and 726  $\text{cm}^{-1}$ .

### Initial pH Effect on Removal of RD5

The initial pH effect on RD5 removal efficiency is presented in Fig. 3. In neutral pH, RD5 is in an anionic form in the presence of sulfonic groups. Thus, it has an electrostatic interaction with the surface of magnetite nanoparticles having a positive surface charge. Thus, negative ions of RD5 can adsorb to the positive surface of  $\text{Fe}_3\text{O}_4@\text{PANI}$ . But in the solutions, with the increasing pH, the negative charge (-OH) on the  $\text{Fe}_3\text{O}_4@\text{PANI}$  increases causing repulsion between  $\text{Fe}_3\text{O}_4@\text{PANI}$  and RD5 and decreases the amount of adsorption. From this, we could conclude that pH = 7 is an optimum pH for the removal of RD5 from the water.

### Effect of Adsorbent Mass on the Removal of RD5

According to Fig. 4, the removal rate of RD5 was increased by keeping the RD5 concentration constant and increasing the  $\text{Fe}_3\text{O}_4@\text{PANI}$  content, so that at optimum pH by increasing the amount of  $\text{Fe}_3\text{O}_4@\text{PANI}$  from 5 to 20 mg, the removal efficiency of the RD5 at a concentration of 30  $\text{mg l}^{-1}$  increased from 40% to 100%. This is due to an increase in the active site on the surface of  $\text{Fe}_3\text{O}_4@\text{PANI}$  due to the rise in the amount of  $\text{Fe}_3\text{O}_4@\text{PANI}$ . Basically, with the increasing surface of  $\text{Fe}_3\text{O}_4@\text{PANI}$ , its specific surface area has been increased, and RD5 molecules have the most possibility of sitting on the  $\text{Fe}_3\text{O}_4@\text{PANI}$  surface. The results show that by increasing the amount of  $\text{Fe}_3\text{O}_4@\text{PANI}$  beyond 20 mg, the percentage removed decreases.

### Temperature Effect on Adsorption Process

The removal of RD5 experiments was carried out at 25, 30, 40, 50 and 60  $^{\circ}\text{C}$ , and the results are presented in Fig. 5. Conforming to the figure, the optimum temperature for the elimination of RD5 from water is 25  $^{\circ}\text{C}$ .

Temperature has a significant effect on the adsorption process. On the one hand, increasing the temperature decreases the diffusion rate of RD5 molecules on the outer and inner layers of the  $\text{Fe}_3\text{O}_4@\text{PANI}$ , and also reduces the viscosity of the solution. On the other hand, the influence of temperature in the process of adsorption provides us information on enthalpy changes and adsorption entropy. In general, increasing the temperature increases the movement of RD5 molecules on the surface. Thus, the adsorption process is slower resulting in less surface covering.

### Ionic Strength Effect on Adsorption Process

The effect of ionic strength on adsorption capacity was investigated by increasing sodium chloride in the range of 0-5% percent. The results are shown in Fig. 6. The results show that with the increasing salt concentration, the RD5 removal decreases.

The salt molecule would prevent the effective interaction of the surface with the RD5 structures by forming a coating layer on the surface of the  $\text{Fe}_3\text{O}_4@\text{PANI}$ . Therefore, salt was not added to the other experiments.

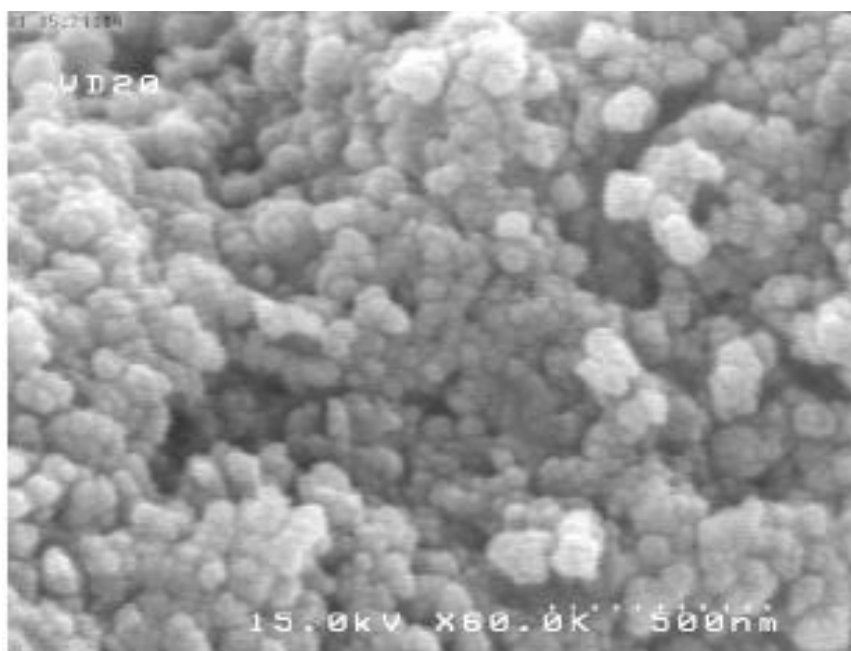
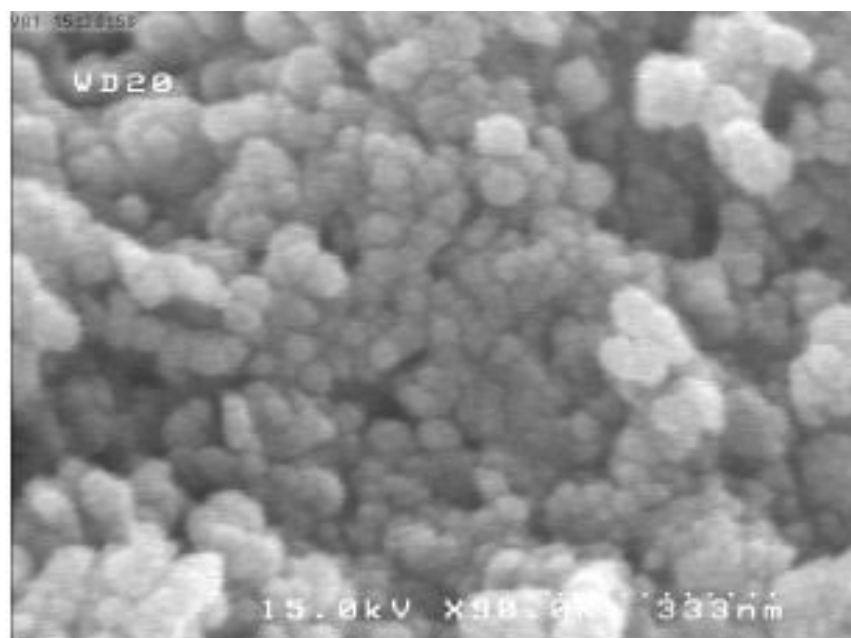


**Fig. 2.** a) SEM images b) XRD pattern and c) FT-IR spectra of  $\text{Fe}_3\text{O}_4$ .

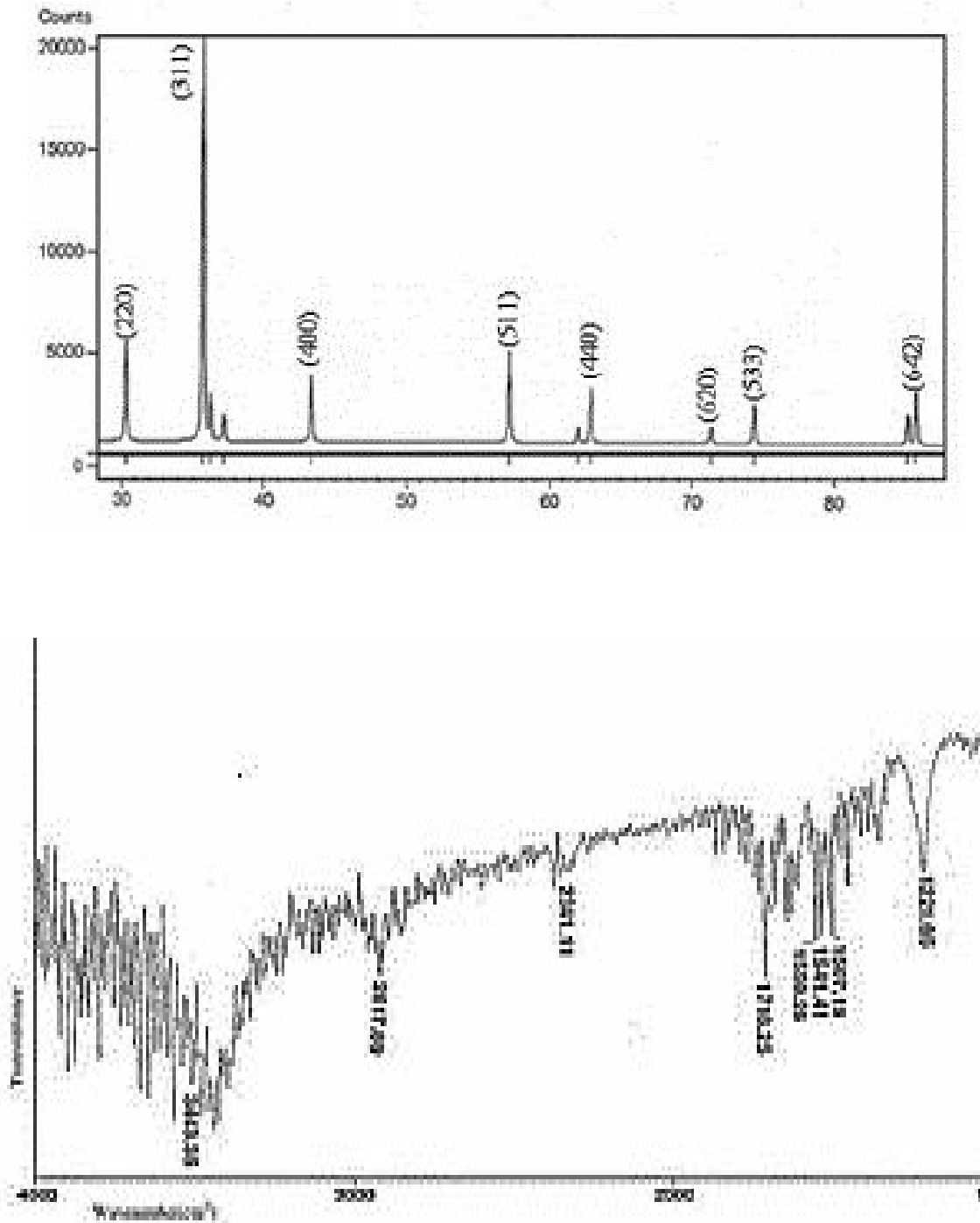
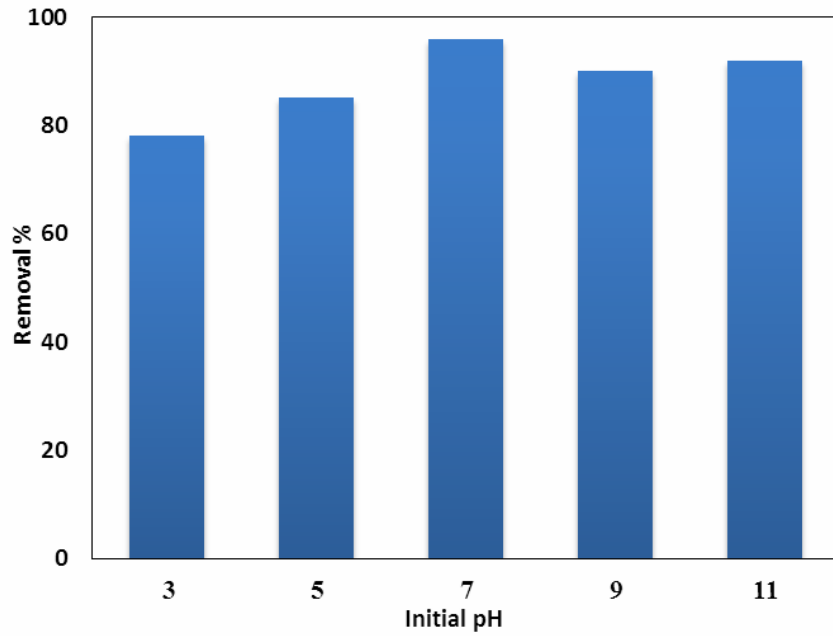
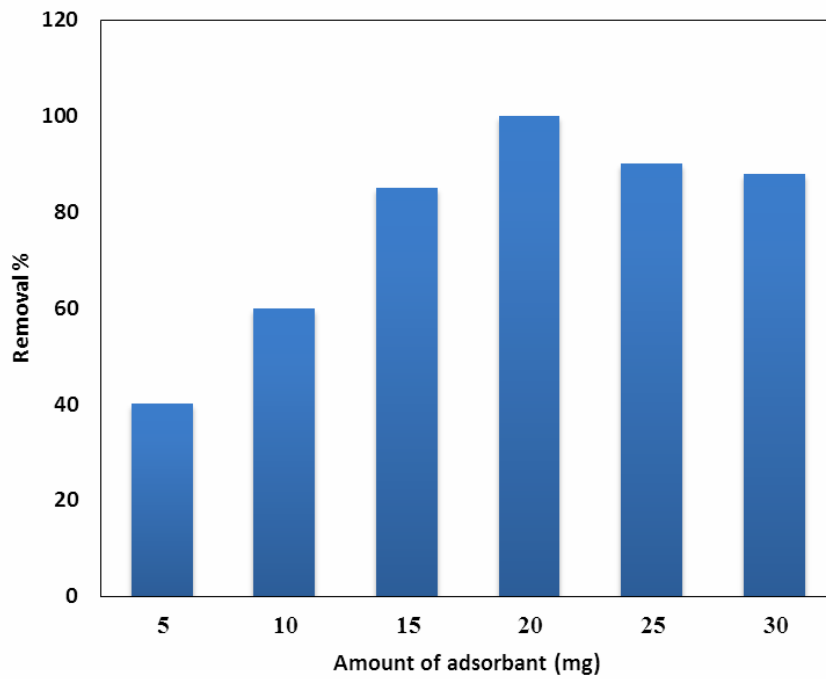


Fig. 2. Continued.



**Fig. 3.** pH effect on RD5 removal efficiency, under conditions: 10 ml of RD5 solution with a concentration of  $30 \text{ mg l}^{-1}$  and 20 mg of adsorbent and contact time: 5 min.



**Fig. 4.** The effect of adsorbent mass on RD5 removal efficiency (concentration of RD5:  $30 \text{ mg l}^{-1}$ , pH = 7, stirring time: 5 min).

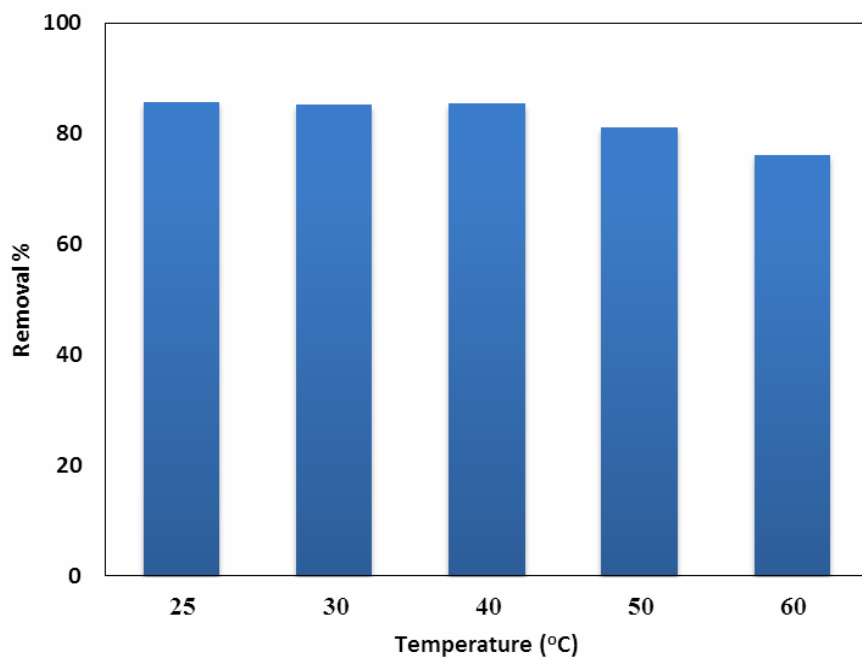


**Fig. 5.** The effect of the temperature on the RD5 removal efficiency. (concentration of RD5: 30 mg l<sup>-1</sup>, pH = 7, stirring time: 5 min).

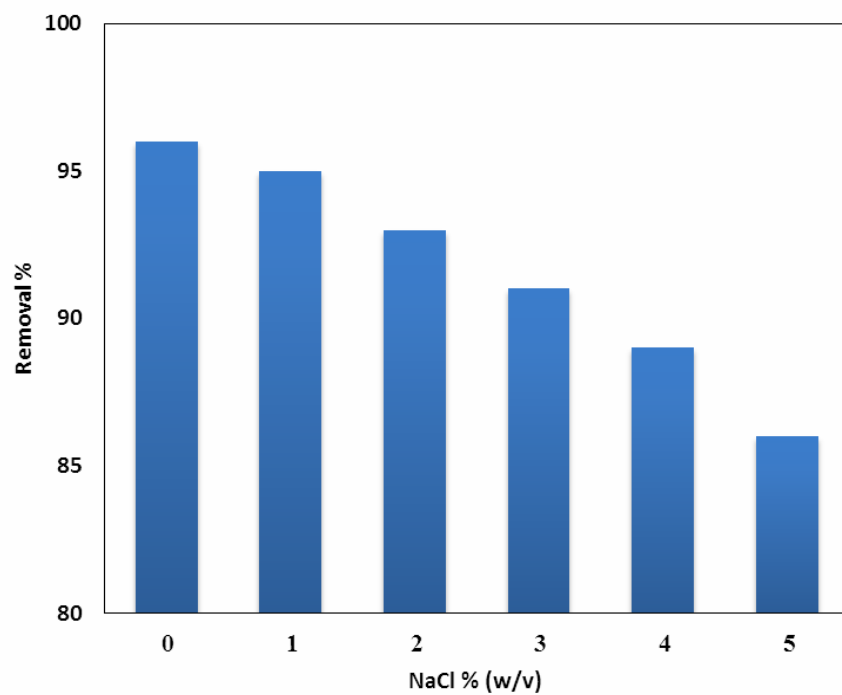


**Fig. 6.** The effect of the ionic strength on the RD5 removal efficiency. (Concentration of RD5: 30 mg l<sup>-1</sup>, pH = 7, stirring time: 5 min).

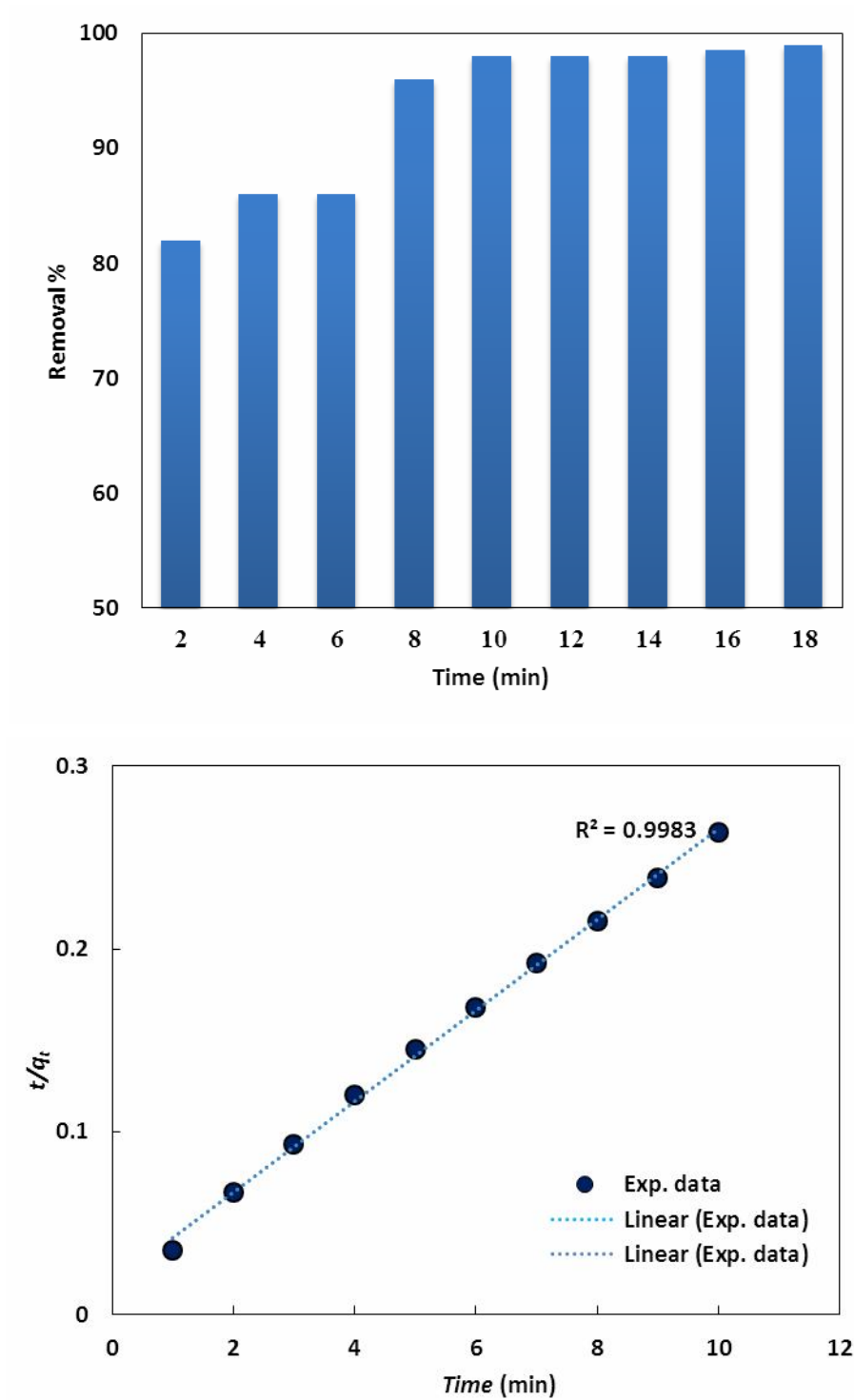


**Fig. 7.** a) The kinetics of the adsorption (concentration of RD5:  $30 \text{ mg l}^{-1}$ , pH = 7, stirring time: 5 min) and b) The pseudo-second order fitting curve with experimental data.

### Effect of Contact Time (Kinetic Study)

The contact time between Fe<sub>3</sub>O<sub>4</sub>@PANI and RD5 is one of the most critical design parameters that affect the process performance. As the Fe<sub>3</sub>O<sub>4</sub>@PANI has a high surface area, high removal capacity, and the fast removal dynamics, the adsorption time is in the range of 1-18 min. The results obtained in Fig. 7a show that the adsorption of RD5 at the concentration of 30 ppm is very fast. Such a high adsorption rate can be due to the lack of high penetration of RD5 in the adsorbent surface because the adsorption occurs only on the surface of the nanoparticles. The equilibrium contact time, comparing to Fig. 7a is around 10 min.

As it was seen, within 10 min, the RD5 adsorption reached its maximum value. Kinetic experiment data were fitted to the pseudo-first and second order reaction rate and according to the correlation coefficient of fitting (see Fig. 7b and Table 1), the pseudo-second reaction order fits very well with experimental data.

Isothermal study of RD5 adsorptionThe most common method for determining adsorption isotherms is to determine the concentration of the species in the solution before and after the experiment. Two isotherm equations in this study, namely, Freundlich and Langmuir adsorption, have been tested to describe the adsorption equilibrium properties. The results obtained for the adsorption isotherm of RD5 were tabulated in Table 3 as shown in Fig. 8.

The results of Table 2 show that the Langmuir model provides a better fitting with adsorption data than the Freundlich model (with close to one correlation coefficients ( $R^2$ )). The maximum adsorption capacity for adsorbent based on the Langmuir model is 63.69 mg g<sup>-1</sup>.

In Table 3, the adsorption capacity of this study was compared with other adsorption capacities reported in literature. Conforming to the Langmuir model, the maximum RD5 adsorption capacity was 63.69 mg g<sup>-1</sup>. Following our results, the adsorption process by designed Fe<sub>3</sub>O<sub>4</sub>@PANI is an efficient and affordable method for eliminating RD5 from the textile industry.

### Thermodynamic Study of Adsorption System

Thermodynamic parameters such as Gibbs free energy, enthalpy, and entropy of the adsorption will be obtained by plotting the  $\ln K$  vs.  $1/T$  at different temperatures. Results were presented in Table 4 and Fig. 9.

Given that  $\Delta G^0$  is negative at all temperatures, we could conclude that the adsorption process is spontaneous. The negative value of  $\Delta H^0$  is an acceptable reason that the adsorption is exothermic.

### Kinetic Study of the Adsorption

If the transfer of RD5 molecules from the bulk to the liquid film or the boundary around the adsorbent is ignored, the RD5 adsorption mechanism consists of the following sequential steps.

1. The transfer of RD5 molecules from the boundary films to the outer surface of the Fe<sub>3</sub>O<sub>4</sub>@PANI (film release).
2. The transfer of the RD5 molecule from the Fe<sub>3</sub>O<sub>4</sub>@PANI surface to the interior of the particles.
3. Adsorption of the RD5 molecules by adsorbent's active sites.

According to Weber and Maurice, if penetration inside the particle is a speed controlling factor, adsorption of Fe<sub>3</sub>O<sub>4</sub>@PANI changes with the square of time. Therefore, the measurement of the RD5 adsorption rate is possible by measuring the adsorption capacity of Fe<sub>3</sub>O<sub>4</sub>@PANI as a second root function of time. The following equation can represent the particle diffusion model:

$$q_t = k_3 t^{1/2} + C \quad (10)$$

Where  $k_3$  [mg g<sup>-1</sup> min<sup>1/2</sup>] is a rate constant of penetration inside the particles. The value of  $k_3$  is obtained by the slope of the straight line of the  $q_t$  graph vs.  $t^{1/2}$ . The  $C$  value provides evidence of the thickness of the boundary layer and, for a larger  $C$  value, the effect of the boundary layer is greater. Fig. 10 shows the diffusion plot inside the particle. In the diagram, there may be two separate regions that represent the steps during the adsorption process. The first curvature is due to the bulk diffusion and the linear section because of the diffusion.

As you can see, the RD5 has not straight-line plot and does not pass from the origin. One of the possible reasons for deviation from the straight line of origin is that there is a difference in the rate of mass transfer at the initial and final stage of RD5 adsorption. The results of this experiment show that intrinsic penetration is not the only control of RD5 adsorption. The rate constant of the particle diffusion model have been tabulated in Table 5.

**Table 1.** Kinetic Parameters of RD5 Removal from Water

Model	$C_0$ (mg l <sup>-1</sup> )	$q_{e,exp}$ (mg g <sup>-1</sup> )	$q_{e,cal}$ (mg g <sup>-1</sup> )	Rate constant	R <sup>2</sup>
Pseudo second order	40	37.8	40.16	$k_2$ (g mg <sup>-1</sup> min <sup>-1</sup> ) = 0.035	0.9984
Pseudo first order	40	37.8	42.52	$k_1$ (min <sup>-1</sup> ) = 0.426	0.9520

**Table 2.** Isotherm Fitted Parameters of RD5 Removal from Water

Langmuir parameters	$K_L$ (l g <sup>-1</sup> )	$q_{max}$ (mg g <sup>-1</sup> )	R <sup>2</sup>
	0.375	63.69	0.998
Freundlich parameters	$K_F$ (l g <sup>-1</sup> )	$n$	R <sup>2</sup>
	25	4.28	0.8449

**Table 3.** Comparison of RD5 Removal with Different Adsorbents Reported in Literature

Adsorbent	Adsorbate	$q_{max}$ (mg g <sup>-1</sup> )	Ref.
Powdered activated carbon	RD5	58.82	[18]
Fly ash (Turkey)	RD5	7.94	[18]
Activated red mud	RD5	35.58	[19]
Polyaniline nanofibers	RD5	312.50	[20]
Banana Peel Powder	RD5	49.20	[21]
This study	RD5	63.69	

**Table 4.** Thermodynamic Parameters of RD5 Removal Process

	$\Delta G^\circ$ (kJ mol <sup>-1</sup> )			$\Delta H^\circ$ (kJ mol <sup>-1</sup> )	$\Delta S^\circ$ (J mol K <sup>-1</sup> )
	298 K	303 K	318 K		
	-4.792	-4.262	-2.672	-28,16	-76.1

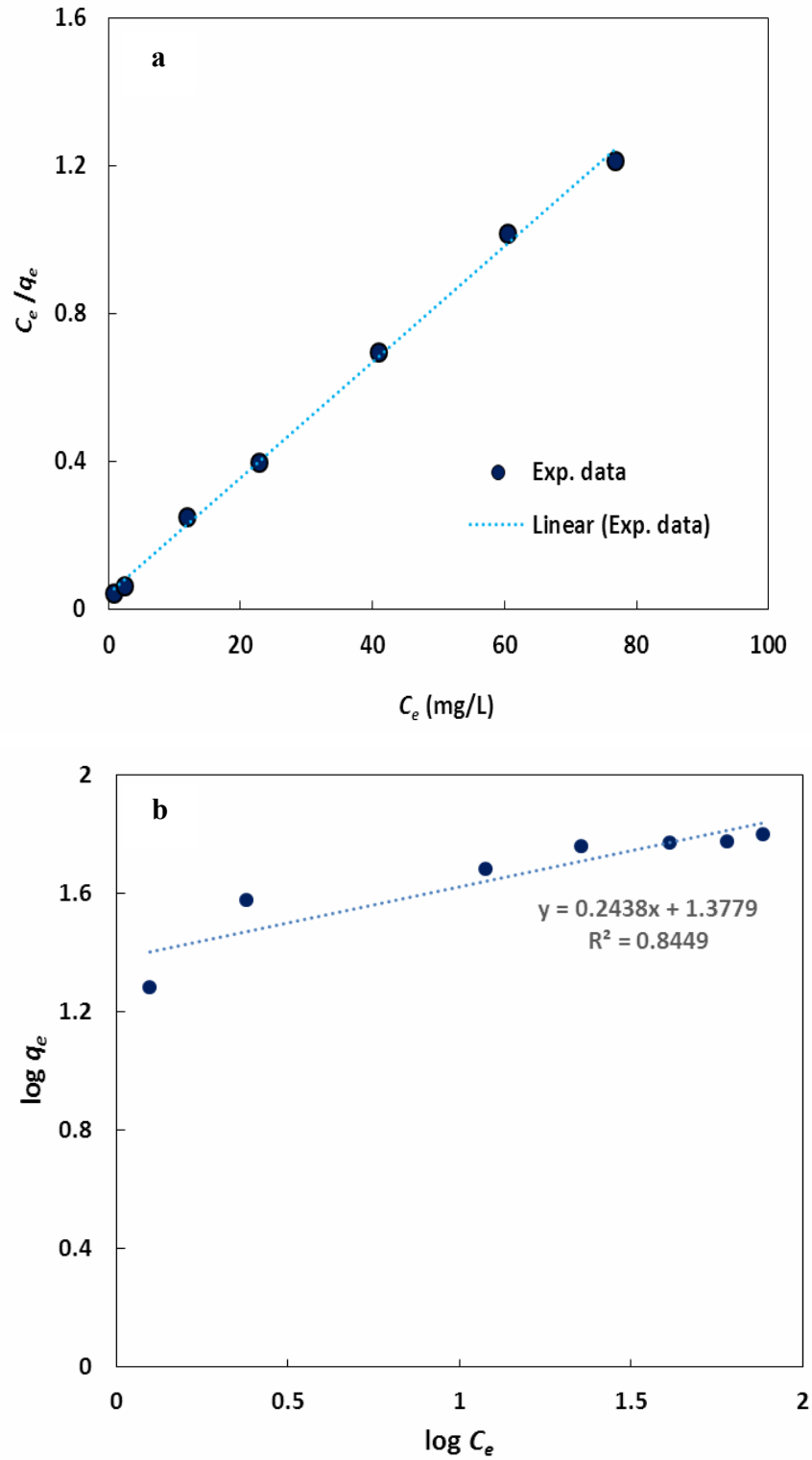


Fig. 8. a) The Langmuir isotherm and b) Freundlich model fitting curve with experimental data.

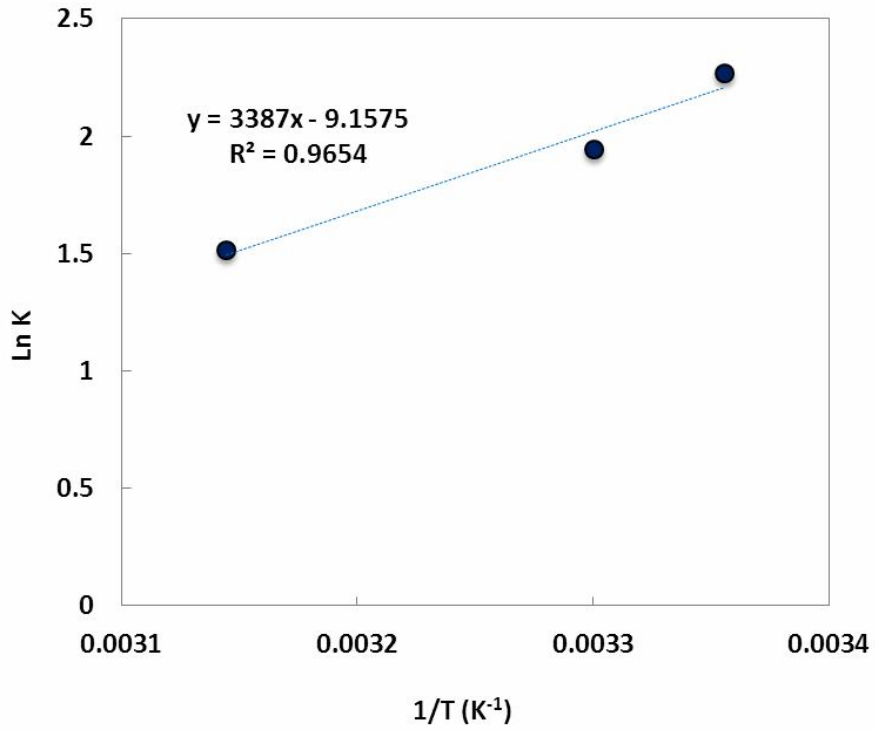


Fig. 9. Obtaining thermodynamic parameters at different temperatures.

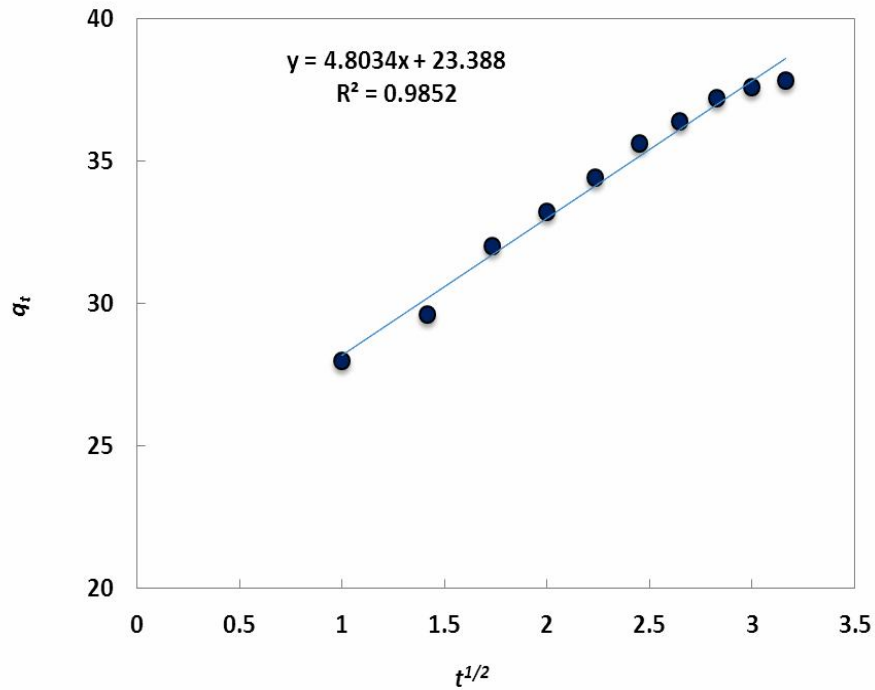


Fig. 10. Diffusion plot inside the particle.

**Table 5.** The Rate Constant of the Particle Diffusion Model

$C_0$ (mg l <sup>-1</sup> )	$k_3$ (mg g <sup>-1</sup> min <sup>-1/2</sup> )	$C$ (mg g <sup>-1</sup> )	$R^2$
40	4.803	23.388	0.9852

## CONCLUSIONS

A magnetic functionalized nanoparticles Fe<sub>3</sub>O<sub>4</sub>@PANI was successfully synthesized and tested in the RD5 elimination. Under optimal conditions, 10 ml of the dye solution with a concentration of 30 mg l<sup>-1</sup>, 20 mg of adsorbent, pH = 7 and contact time of 10 min, there appears color removal of 100%. The results also showed that the adsorption process follows Langmuir isotherm with the regression coefficient of  $R^2 = 0.998$ . In Table 5, the adsorption capacities of this study were compared with other adsorption capacities reported in literature. The maximum RD5 adsorption capacity was 63.69 mg g<sup>-1</sup> conforming to the Langmuir model. Following our results, the adsorption process by designed Fe<sub>3</sub>O<sub>4</sub>@PANI is an efficient and affordable method for eliminating RD5 from the textile industry. Furthermore, taking into account the advantage of the fast and simple magnetic action of the adsorbent through the application of an external magnetic field, the Fe<sub>3</sub>O<sub>4</sub>@PANI can be considered an effective adsorbent for removal of RD5 from the water.

## ACKNOWLEDGMENTS

Authors are grateful to University of Tehran and University of Imam Hossein for the financial support.

## REFERENCES

- [1] Karamipour, A.; *et al.*, A kinetic study on adsorption of congo red from aqueous solution by ZnO-ZnFe<sub>2</sub>O<sub>4</sub>-polypyrrole magnetic nanocomposite. *Phys. Chem. Res.* **2016**, *4*, 291-301, DOI: 10.22036/pcr.2016.14114.
- [2] Rostamian, R.; Najafi, M.; Rafati, A. A., Synthesis and characterization of thiol-functionalized silica nano hollow sphere as a novel adsorbent for removal of poisonous heavy metal ions from water: Kinetics, isotherms and error analysis. *Chem. Eng. J.* **2011**, *171*, 1004-1011, DOI: 10.1016/j.cej.2011.04.051.
- [3] Rostamian, R.; Behnejad, H., A unified platform for experimental and quantum mechanical study of antibiotic removal from water. *J. Wat. Proc. Eng.* **2017**, *17*, 207-215, DOI: 10.1016/j.jwpe.2017.04.009.
- [4] Ahmad, R.; Mondal, P.K., Application of acid treated almond peel for removal and recovery of brilliant green from industrial wastewater by column operation. *Sep. Sci. Tech.* **2009**, *44*, 1638-1655, DOI: 10.1080/01496390902775836.
- [5] Slokar, Y.; March, A., Majcen Le Marechal. Methods of decoloration of textile wastewaters. *Dyes Pigm.* **1998**, *37*, 335-356, DOI: 10.1016/S0143-7208(97)00075-2.
- [6] Neyens, E.; Baeyens, J., A review of classic Fenton's peroxidation as an advanced oxidation technique. *J. Hazard. Mater.* **2003**, *98*, *1*, 33-50, DOI: 10.1016/S0304-3894(02)00282-0.
- [7] Sohrabi, N.; Rasouli, N.; Alirezaarab, F., Response surface methodology for optimizing adsorption process parameters of amaranth removal using magnetic layer double hydroxide (Fe<sub>3</sub>O<sub>4</sub>/ZnFe-LDH). *Phys. Chem. Res.* **2019**, *7*, 131-148, DOI: 10.22036/pcr.2018.152521.1548.
- [8] Ertugay, N.; Acar, F.N., Removal of COD and color from Direct Blue 71 azo dye wastewater by Fenton's oxidation: Kinetic study. *Arab. J. Chem.* **2017**, *10*, S1158-S1163, DOI: 10.1016/j.arabjc.2013.02.009.
- [9] Mouni, L.; Belkhir, L.; Bollinger, J.C.; Bouzaza, A.; Assadi, A.; Tirri, A.; Remini, H., Removal of

- methylene blue from aqueous solutions by adsorption on Kaolin: Kinetic and equilibrium studies. *Appl. Clay Sci.* **2018**, *153*, 38-45, DOI: 10.1016/j.clay.2017.11.034.
- [10] Hamedani, S.; Felgari, Z., Adsorption properties of folic acid onto functionalized carbon nanotubes: isotherms and thermodynamics studies. *Phys. Chem. Res.* **2017**, *5*, 519-529, DOI: 10.22036/pcr.2017.78175.1359.
- [11] De Gisi, S.; Lofrano, G.; Grassi, M.; Notarnicola, M., Characteristics and adsorption capacities of low-cost sorbents for wastewater treatment: A review. *Sus. Mat. Tech.* **2016**, *9*, 10-40, DOI: 10.1016/j.susmat.2016.06.002.
- [12] Kolhatkar, A.; Jamison, A.; Litvinov, D.; Willson, R.; Lee, T., Tuning the magnetic properties of nanoparticles. *Int. J. Mol. Sci.* **2013**, *14*, 15977-16009, DOI: 10.3390/ijms140815977.
- [13] Thue, P. S.; *et al.*, Synthesis and characterization of a novel organic-inorganic hybrid clay adsorbent for the removal of acid red 1 and acid green 25 from aqueous solutions. *J. Clean Prod.* **2018**, *171*, 30-44, DOI: 10.1016/j.jclepro.2017.09.278.
- [14] Chowdhury, A. N.; Jesmeen, S. R.; Hossain, M. M., Removal of dyes from water by conducting polymeric adsorbent. *Polym. Adv. Technol.* **2004**, *15*, 633-638, DOI: 10.1002/pat.521.
- [15] Pandey, G.; Singh, S.; Hitkari, G., Synthesis and characterization of polyvinyl pyrrolidone (PVP)-coated Fe<sub>3</sub>O<sub>4</sub> nanoparticles by chemical co-precipitation method and removal of Congo red dye by adsorption process. *Int. Nano Lett.* **2018**, *8*, 111-121, DOI: 10.1007/s40089-018-0234-6.
- [16] Sydoruk, V.; *et al.*, Activated carbons with adsorbed cations as photocatalysts for pollutants degradation in aqueous medium. *Adsorption.* **2019**, 1-12, DOI: 10.1007/s10450-018-00006-0.
- [17] Skwarek, E.; Janusz, W., Adsorption of Ba<sup>2+</sup> ions at the hydroxyapatite/NaCl solution interface. *Adsorption*, **2019**, *1*, 1-12, DOI: 10.1007/s10450-018-00005-1.
- [18] Eren, Z.; Acar, F. N., Adsorption of reactive black 5 from an aqueous solution: equilibrium and kinetic studies. *Desalination*, **2006**, *194*, 1-10, DOI: 10.1016/j.desal.2005.10.022.
- [19] Shirzad-Siboni, M.; Jafari, S. J.; Ghihi, O.; Kim, I.; Lee, S. M.; Yang, J. K., Removal of acid blue 113 and reactive black 5 dye from aqueous solutions by activated red mud. *J. Indust. Eng. Chem.* **2014**, *20*, 1432-1437, DOI: 10.1016/j.jiec.2013.07.028.
- [20] Bhaumik, M.; McCrindle, R. I.; Maity, A.; Agarwal, S.; Gupta, V. K., Polyaniline nanofibers as highly effective re-usable adsorbent for removal of reactive black 5 from aqueous solutions. *J. Colloid Interface Sci.* **2016**, *466*, 442-451, DOI: 10.1016/j.jcis.2015.12.056.
- [21] Munagapati, V. S.; Yarramuthi, V.; Kim, Y.; Lee, K. M.; Kim, D. S., Removal of anionic dyes (Reactive black 5 and Congo red) from aqueous solutions using banana peel powder as an adsorbent. *Ecotox. Environ. Safe.* **2018**, *148*, 601-607, DOI: 10.1016/j.ecoenv.2017.10.075.